Micropinch in a high-current diode

E. D. Korop, B. É. Meĭerovich, Yu. V. Sidel'nikov, and S. T. Sukhorukov

I. V. Kurchatov Institute of Atomic Energy, Moscow,
Institute of Physical Problems, Academy of Sciences of the USSR,
Institute of Spectroscopy, Academy of Sciences of the USSR,
and Institute of Theoretical and Experimental Physics, Moscow
Usp. Fiz. Nauk **129**, 87–112 (September 1979)

The basic data on the micropinch in a high-current, low-inductance spark are reviewed. This phenomenon was discovered by Cohen *et al.* in 1968. A theory for the equilibrium and collisionless emission of a plasma compressed to a degenerate state by the magnetic field of the high current yields a natural explanation for several properties of the micropinch which are unexpected at first glance: the hard x-ray burst, the time evolution and directional pattern of this burst, the power-law spectrum above 150 keV, the confinement of the emission sources to certain spatial regions, and the highly ionized atoms, among others. (Similar effects are observed in z pinches, the plasma focus, and the explosion of wires.) At maximum compression, the micropinch seems to be similar to the Thomas-Fermi "linear atom," which consists of ions which are at rest on the whole and drifting electrons which carry the current. The micropinch has potential applications (in the fusion problem and in developing sources of induced synchrotron radiation for the x-ray range), but it is also of much physical interest in itself, since it allows laboratory research on a supercontracted hot plasma, i.e., matter in a state approaching that in stars. In order to prove unmistakably that supercontracted matter is present in a micropinch, however, it would be necessary to carry out direct experiments to observe the strong electromagnetic fields and the high density of matter in regions with dimensions measured in angstroms.

PACS numbers: 52.55.Ez, 52.25.Ps, 52.25.Lp

CONTENTS

1. INTRODUCTION

One of the most interesting effects which have been observed in sparks, in our opinion, is the formation of a micropinch region in which the state of the matter approaches that in stars, discovered in 1968 by Cohen *et al.*[1] in experiments with a low-inductance vacuum spark. Levedev *et al.*,[2] Plyutto *et al.*,[3,4] and Händel *et al.*[5,6] all came close to discovering this unique property of sparks. Today we also know that the physical nature of this effect has much in common with that of the plasma focus of Filippov[7] and Mather.[8] Our major purpose in this paper is to review the present state of experimental research and the theory regarding the physical nature of the micropinch.

The first scientific conference on spark discharges was held near the end of the last century,[9] just after the discovery of x rays. At the time, physicists had probably not yet run into this phenomenon, which, although very interesting from the experimental standpoint, is very awkward to deal with theoretically. The situation was such that, despite constant study of the nature of the spark for more than half a century, not a single one of the properties of sparks which were observed experimentally had been predicted theoretically beforehand (among these properties are the x-ray burst,[9] the high temperature and the multiple ionization of atoms,[10] self-contracted electron beams,[11] fast ions,[12] and the explosive nature of the electron emission[13,14]). Research of recent years has shown that we still have

 0038-5670/79/090727-15$01.10 © 1980 American Institute of Physics

much to learn about this type of discharge, although the spark is nearly the most common type of naturally occurring discharge.

By "spark" we mean a brief stage (lasting ~10^{-7} sec, according to experiments) in the formation of those conditions which are required for a stable arc.[15] Clearly, all types of vacuum breakdown, including the explosive emission in the diodes of high-current electron accelerators,[16-18] are sparks. Events characteristic of sparks also precede the establishment of an electric arc at atmospheric pressure.[19-21]

In addition to reviewing the standard concepts here, we shall outline a nontraditional approach to the theory of the micropinch, based on an analysis of the equilibrium of a plasma in the magnetic field produced by the current.[22] The results show that conditions can be created in the course of the micropinch such that the magnetic forces due to the current compress the hot plasma to the point of electron degeneracy, i. e., to a condensed state. At maximum compression, the micropinch is similar to a Thomas–Fermi "linear atom," consisting of ions which are at rest on the whole and drifting electrons which carry the current. This state of matter, which has never arisen before, would seem to be a unique example of a macroscopic quantum object[23] at high temperatures. The emission observed experimentally can be explained in a natural way as the collisionless emission resulting from electron transitions between quantum levels in the course of the filling of the states of the linear atom[24] and the subsequent radiative cooling of this linear atom.

2. EXPERIMENTAL RESEARCH ON MICROPINCHES

(a) Apparatus for spark research

The micropinch in a vacuum arc is today the object of widespread study. Until recently, the only motivation for this research came from spectroscopic applications, i. e., the need for a laboratory source of x-ray spectra comparable to stellar spectra. It is thus not surprising that most of the work was concentrated on the same aspects of the effect, and the experimental conditions were pretty much the same. We will describe only one particular experimental device here, but this is apparently not the only device in which a micropinch region could be created.

The experimental arrangement is shown in Fig. 1a. A spark is produced between cathode 2 and anode 3 in a vacuum gap ≤ 1 cm in size, either by a low-energy discharge (10–30 J) at the central part of the cathode or by a laser beam focused on the anode surface (Fig. 1b). In the laser case, the laser beam passes through a hole ~2 mm in diameter in the cathode and can partially vaporize the material around the hole. The anode is a protruding cone with a vertex angle ~90°. The vapor of the anode material usually produces a spectrum of highly ionized atoms. Various metals are used as anode (Ti, Fe, Ni, Cu, Mo, and W), while the cathode is usually made of stainless steel. Electrodes 2 and 3 are connected to a capacitor bank either directly or through a controlled switch. If the bank is initially charged to

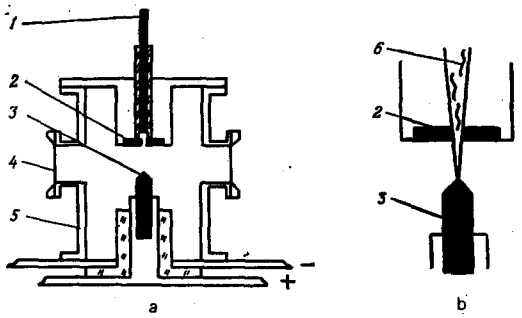

FIG. 1. Experimental arrangement for studying the micropinch. a: 1) Trigger electrode; 2) cathode; 3) anode; 4) diagnostic window; 5) vacuum chamber. b: Laser ignition. 6) Laser beam focused through an aperture in the cathode onto the anode.

~10–15 kV, the energy stored in it is ~1–2 kJ. Vacuum chamber 5, with diagnostic windows 4, serves as the return conductor. The coaxial electrode geometry minimizes the circuit inductance: $\lesssim 10^{-7}$ H. Variations in the residual gas pressure over the range 10^{-3}–10^{-6} torr do not significantly affect the characteristics of the spark[25] or the properties of the micropinch region.

The discharge current and the emission in various parts of the spectrum, from the microwave region (10–20 GHz) to the region of hard x rays (100–500 keV), carry information about the properties of the micropinch. Particularly valuable results have been obtained from a study of the variation of the x-ray emission over space and time and from a study of the x-ray spectrum. The techniques which have been used will be discussed below in connection with the description of the corresponding experiments. We might note that the electromagnetic noise level is high, and it forces the experimentalist to be very careful in the electrical measurements and to use great caution in drawing conclusions from these measurements.

(b) Current characteristics

The current and its time derivative are measured by means of a Rogowski loop with a time resolution $\lesssim 10^{-8}$ sec. The discharge current, a damped sine wave, reaches a maximum amplitude of ~100–200 kA in ~(1.5–2) $\times 10^{-6}$ sec. We can take the spark stage to be the first quarter-period of the current, and we can arbitrarily break this stage up into two substages. The "starting" or "breakdown" substage ends with the filling of the vacuum gap by the plasma bursts from the anode and the cathode[14,26] and the decay of the voltage to a level approximately equal to the potential drop across the inductance of the current channel. The diodes of high-current electron accelerators are essentially operating in this starting substage. The explosive emission of the cathode,[14] the formation of electron beams in the cathode burst, and the acceleration of ions of the cathode material[27] are some of the basic events which occur in this substage, and they largely determine the transient effects which culminate in a high conductivity in the diodes.

In the second substage, the rate of increase of the

current is limited, for the most part, by the circuit inductance. This substage can be called the "unstable arc substage." Its most characteristic features are brief drops in the current (lasting $\lesssim 10^{-7}$ sec), which are accompanied by overvoltage pulses: these pulses sometimes exceed the initial voltage across the diode by a factor of two or three. At the same time, there are intense bursts of emission. In contrast with the starting substage, in which it is primarily the anode which is radiating, the primary source of the x rays in the second substage consists of the discharge channel[6] and the micropinch region in the dense vapor of the anode material.[1,29] In this substage, as in the starting substage, self-contracted electron beams are observed, and ions are observed to be accelerated toward the anode.[12,28,30] Similar x-ray bursts are observed from a plasma focus, whose formation near an anode is also accompanied by drops in the discharge current.[7,8]

The discharge current does not fall by more than 30% from its value at the instant of the drop.[31] These current drops (of which there may be several[32]; Fig. 2a) are random in nature, although many investigators report that the time at which they occur depends on the conditions under which the discharge was produced, the circuit parameters, and the electrode shape and material.[31,33,34] After the current maximum–more precisely, after the last x-ray burst–an arc is established.[2,15]

(c) Emission from the micropinch region

These drops in the current are accompanied by bursts of emission over a broad spectral range, from the microwave region to the hard x-ray region (Fig. 2).

1) Microwave and infrared emission

The submillimeter emission from the plasma of a vacuum diode was observed in Refs. 32 and 35. Absolute values of the emission intensity were not measured. At present, there have been no time-resolved directional measurements of the microwave emission of vacuum diodes. Under these circumstances, there is accordingly much interest in the corresponding measurements for the plasma focus. Herziger *et al.*[36] have reported directional patterns of the microwave emission from a plasma focus. Their measurements showed that there are two types of microwave emission, which are separated in time and which have different directional patterns. Figure 3a shows directional patterns of the microwave emission at the beginning of the burst, while Fig. 3b shows the corresponding results for the final stage of the emission.[36] The emission intensity here is[36] ~1 W. At present, these are the only results which have been reported on the directional pattern of the microwave emission; confirmation of the results of Ref. 36 would be desirable.

An intensification of the infrared emission in the region 0.7–1.2 μ was observed in Refs. 31 and 34. Interpreting this emission as the emission from the micropinch at twice the plasma frequency, Cilliers *et al.*[31] and Turechek and Kunze[34] estimated the electron density in the plasma to be $n_e \sim (1-5)\times 10^{20}$ cm^{-3}. In terms of the theory which will be discussed below, the emission from the micropinch (this includes the microwave emission, in particular) can be interpreted as emission due to the motion of electrons along finite trajectories in a collective interaction field.

2) Visible emission

Lee and Elton[33] studied the emission in the visible region. They detected the light by using electron-optical image converters with a continuous time sweep of the image, synchronized with measurements of the discharge current. It was concluded from their observations that the micropinch region is formed at the front of an anode plasma which is propagating toward the cathode at $(0.5-1)\times 10^6$ cm/sec. This velocity of the visible boundary of the anode plasma increases just before the drops in the current. During the x-ray burst, this emission boundary suddenly reverses direction and moves back toward the anode. The characteristic velocity of the fast motions is 10^7–10^8 cm/sec, but the velocity of the micropinch region along the discharge is no more than 10^6 cm/sec.

3) X-ray emission

Händel *et al.*[5,6] observed x-ray emission from the discharge channel over the entire length of this channel. The most intense emission occurs near the anode at the time corresponding to the minimum value of the derivative of the current at a current drop. The intensity of the x-ray burst and the relative hardness of this burst both increase with increasing value of the current at the time of the drop.[33] As the x-ray energy increases,

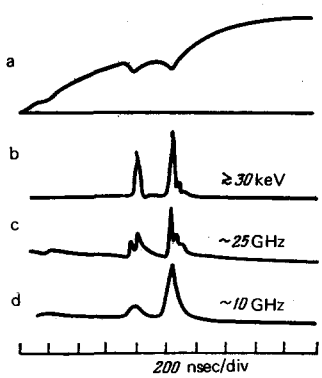

FIG. 2. Time evolution of various properties. a) The current; b) the intensity of hard x rays; c, d) Intensity of the submillimeter emission.[32]

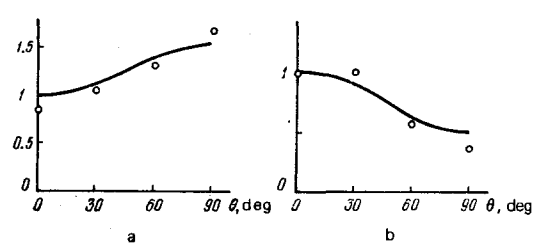

FIG. 3. Directional patterns of the microwave emission of the plasma focus.[36] a) During the burst; b) in the final stage of the emission. Circles) Experimental[36]; curves) plotted from Eqs. (13) (a) and (9) (b).

the duration of the emission falls off[6,31,32] (Fig. 4). The observed intensity of the hard x-ray emission at x-ray energies ≳100 keV falls off by a power law[32,33] (Fig. 5). The x rays which have been detected have had energies ≳1 MeV (Ref. 32). At energies <100 keV, the spectrum corresponds to the emission of a plasma with a temperature ~10 keV, averaged over space and time.[32]

A better time resolution was achieved in the x-ray range in Ref. 31 with the help of a monochromator. It can be seen from Fig. 6 that the emission in the line corresponding to the resonant transition of the helium-like iron atoms begins 3 nsec after the burst at the broadened $K\alpha$ line and ends after 10 nsec. The x rays with energies >10 keV appear after an even shorter delay (1 nsec). The length of this signal at half-maximum is ≲3 nsec. The possibility of separate x-ray bursts was studied in Refs. 31, 37, and 38, but distinct bursts were not time-resolved.

In special experiments carried out to determine the region in which the $K\alpha$ line was excited it was found that in the stage of the current drops, in which there is intense ionization of the anode plasma and a micropinch appears, no $K\alpha$ line is detected from the anode.[31] The implication is that the region of intense ionization is away from the anode; this suggestion agrees with the results of Refs. 33 and 39.

Herziger *et al.*[40] observed a strong angular anisotropy in the soft x-ray emission ($\hbar\omega = 1-1.5$ keV) of a plasma focus of the Mather type. The voltage across the circuit capacitance was 10 kV, and the energy stored in the capacitance was 1 kJ; the diameters of the outer and inner electrodes were 18 and 6 mm; these electrodes were both 40 mm long; and the initial hydrogen pressure was 7 torr. The angular separation of the apertures in the screen was 70 mrad. It was found that the x-ray emitting region lies near the axis above the hollow anode and has a complex structure. The x rays from the various individual sources pass primarily through only a single aperture in the screen. Then the angular divergence is less than 70 mrad. According to Turechek and Kunze,[34] the pronounced angular anisotropy is a consequence of the induced emission of a large number of electrons which have been accelerated to relativistic energies and which are moving in a structure with a periodic density, which may arise because two-stream instabilities are driven in the plasma.

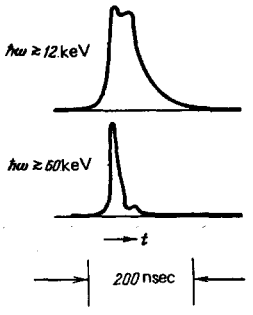

FIG. 4. Time evolution of the emission intensity for various x-ray energies.[32]

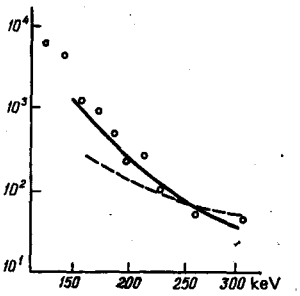

FIG. 5. Variation of the intensity of the emission of the hard x rays with their energy. Circles) Experimental[32]; solid curves) power-law decay of the intensity with an exponent of 4.5; dashed curve) the same, with an exponent of 2.5.

4) *Multiply ionized ions.*

The emission from the micropinch region was studied in Refs. 1, 27–29, 37, 39, 41, and 42 in order to determine the spectra of ions with a high charge. The interest in the spectroscopy of multiply charged ions stemmed from the need to be able to identify the lines in solar flares and in fusion devices. Figure 7 shows a typical spectrum of iron ions[37] over the interval 1.7–1.95 Å. The micropinch spectrum contains lines corresponding to resonant transitions of hydrogen-like ($\lambda \sim 1.85$ Å) iron ions and their satellites. The most intense lines are of the K spectra of Fe II and the ions Fe IX–Fe XVIII, but these lines are emitted from regions adjacent to the micropinch.[39] Figure 8 shows a spectrum[37] in the region of the $K\beta$ line of Fe and the corresponding line from an x-ray tube. The blue shift of the spectrum is evidence of the high degree of ionization in the spark plasma.

Figure 9 compares part of the spectrum of a vacuum spark with the corresponding data from a solar flare.[42] The same type of pronounced line broadening in comparison with the solar spectrum is observed in the spectra of exploding wires.[43] The observed broadening of the micropinch lines can be attributed to the Doppler, Zeeman, and Stark effects. If it is assumed that the Doppler broadening is caused by the thermal velocity

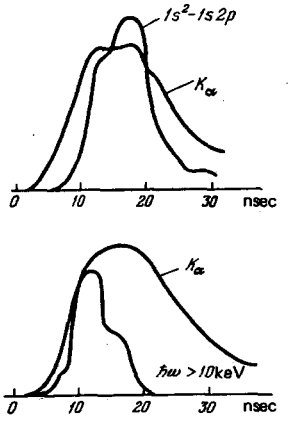

FIG. 6. Intensity of the emission of the helium-like line of iron, the $K\alpha$ line, and the hard x-ray component.[31]

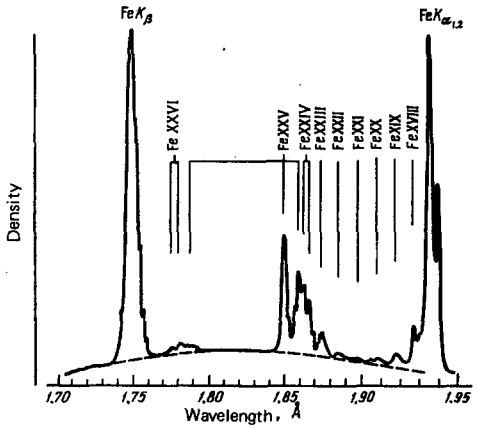

FIG. 7. Spectra of iron ions with various charges.[37]

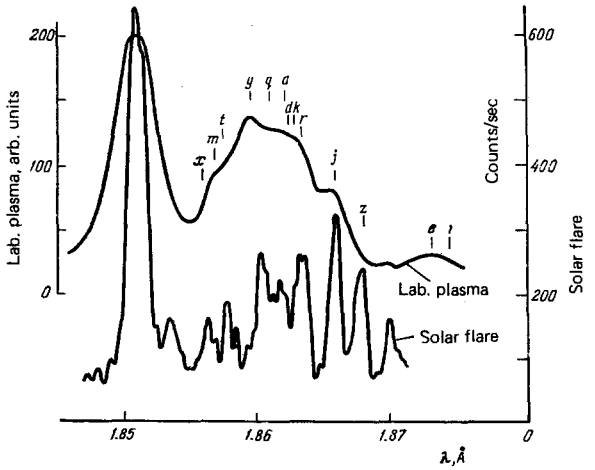

FIG. 9. Part of the spectrum of the vacuum spark and the corresponding part of the spectrum of a solar flare.[42]

spread of the emitting ions, the ion temperature would be estimated[41] to be $T_i \sim 20-40$ keV. If, on the other hand, the Doppler broadening is attributed to directed motion (a contraction or expansion), the ion velocity would be $\sim 4 \times 10^7$ cm/sec. The observed line width might also be attributed to the Zeeman effect, and in this case the magnetic field would have to exceed 10^9 Oe. That there are magnetic fields of 10^8-10^9 Oe in a micropinch follows directly from the fact that the spark radius at currents of the order of 100 kA is[39,41] $r_0 \sim 10^{-4}$ cm. The possibility of fields of the order of 10^9 Oe and higher is discussed by Nardi,[45] who suggests a possible complex spatial structure of the micropinch–a structure which cannot be resolved with the diagnostic apparatus currently available.

If the observed line broadening is attributed to a Stark mechanism, there would have to be electric fields of the order of 10^{14}V/cm. The operation of the Stark mechanism for the broadening of the Lyman series of Al XIII was observed by Datla and Griem.[46] Stark broadening is easily identified, because only in this case does the line width increase with increasing principal quantum number (n) within a single series of spectral lines.

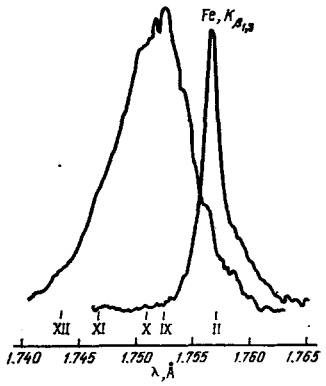

FIG. 8. Spectrum of the plasma of a vacuum spark in the vicinity of the characteristic line $K\beta$ of Fe; the $K\beta$ line of Fe from an x-ray tube. The Roman numerals show the positions of the $K\beta$ line for the ions with various charges.

The detection of lines of resonant transitions and their satellites in hydrogen-like and helium-like ions has made it possible to determine the electron temperature. At the time at which emission of these lines begins, the electron temperature is[37] $T_e = 4.5-5$ keV. Bhalla *et al.*[47] conclude that the ions at the various charge levels are not at an ionizational equilibrium at this electron temperature. The time over which emission occurs in the lines of multiply ionized ions is much longer than the time required for the ions of intermediate size to traverse the micropinch region.[31,37] It can be concluded that the ions are restrained from transverse expansion by the electromagnetic field of a collective interaction.[35]

(d) Ion acceleration

During the current drops, the spark is a source of fast particles. Plyutto *et al.*[12,28,29] have observed an acceleration of the ions in the cathode plasma toward the anode, to energies in the MeV range. At the same time, self-contracted electron beams have been observed to form in the cathode plasma.[30,48,49] Streams of high-energy ions of the anode material have also been observed,[32] and the energy associated with their directional motion toward the cathode has been comparable to the thermal energy in the micropinch (20–40 keV). Lee[32] suggests that a large part of the energy which is evolved in the discharge, primarily in the micropinch, is carried away by this stream of particles. According to observations of a plasma focus,[50,51] the energy of the deuterons in this stream can reach 1–5 MeV, which is much higher than the thermal energy of the deuterons in the focus (~1 keV). Neutron emission is observed at the same time as the current drops.[50-52] To a large extent, these neutrons may be a consequence of the high density and temperature in the plasma focus[53] and the micropinch. The presence of this state of matter follows from the theory discussed below, but it is difficult to actually prove that this state exists on the basis of the experimental evidence presently available.

(e) Structure, spatial position, and time evolution of the micropinch

The dimensions and position of the micropinch have been determined by an x-ray pinhole-camera method.[1,41,46,52,54] The results show that nearly all the x-ray emission during a current drop comes from a region with a longitudinal dimension $L \lesssim 100$ μ (along the discharge axis) and a transverse dimension $d \lesssim 10$–40 μ (Table I). This region is in the vapor of the anode material, ~1 mm from the anode surface. On a finer scale it can be seen that there are inhomogeneities in the x-ray emission.[38,46,55] Figure 10 shows densitometer traces of an x-ray image obtained through 10-μ slits oriented perpendicular to the discharge axis. The slits were covered with foil of various metals (Fe, Mn, and Cr) for which the absorption edges (Fig. 10) fall in different parts of the spectrum of the highly ionized iron atoms (Fe XII-Fe XXV). The foil thicknesses were chosen so as to provide a uniform attenuation of the x-ray emission at the absorption edge for all three slits. It was thus possible to determine the temperatures of the various parts of the micropinch region from the populations of ions with different charge levels. The curves in Fig. 10 are the results of an analysis of a photograph of a single spark. It can be seen that the micropinch consists of a group of clearly defined sources, each of which has a dimension ~20–40 μ along the discharge axis. The sources are separated by regions which are not as bright. It follows from a comparison of the shape of the curves that the source temperature is $\gtrsim 3$ keV, while the temperature in the intervening regions is 1 keV. Usually, one or two groups of sources are observed, on roughly a common axis, which coincides with the discharge axis. The regions between these sources, ~100 μ in size, emit only faintly in the x-ray range.

Analogous structures have been observed in the plasma focus.[40,54] The sources of the harder x rays are smaller in size and are "buried" in a region of softer x-ray emission.

According to the experimental data of Refs. 1, 31–35, 41, 37, 38, 39, and 54 (summarized in Table I), the plasma in the spark has an average density $n_e \sim 10^{21}$ cm^{-3} and a temperature $T_e \sim 10$ keV. The relaxation time due to Coulomb collisions is $\tau_0 \sim 0.04$ nsec at this density and this temperature. Figure 11 shows the relaxation time τ_0 plotted against the temperature T_e for various

TABLE I. Properties of the micropinch plasma according to experimental data

Reference and year	T_e, keV	T_i, keV	n, 10^{20} cm^{-3}	r_0, 10^{-4} cm	L, 10^{-4} cm	Burst duration, nsec
[1], 1968	4—6		10^{-2}—10	<15		~100
[33], 1971	2—100		$\gtrsim 1$	<7.5		~100
[41], 1972	~4	~30	~1	2		~50
[35], 1972	30		~20	~10		~50
[54], 1974	2.5		10	8	40	$\gtrsim 20$
[32], 1974	8±2		10	10—25	100	~30
[38], 1975	3				100	
[34], 1975	35	40	5			20
[31], 1975	$\leqslant 15$	$\leqslant 10$	5	40		20
[37], 1977	4.5	20—40	5			
[39], 1977				1.5		20—100

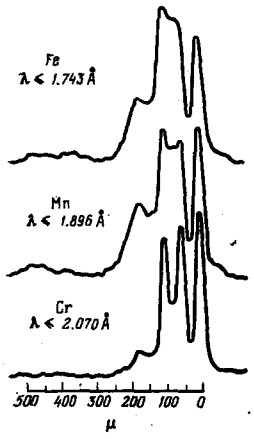

FIG. 10. Densitometer traces of the x-ray image obtained with slits with various filters.[38]

values of the electron density n_e. The points show the plasma properties reported in the experimental papers.[31,32,34,35,37,41] In all these experiments, the relaxation time τ_0 was less than a nanosecond, while the duration of the emission burst ranged from 1 or 2 nsec for the hard x rays to hundreds of nanoseconds in the microwave region. The leading edge of the emission pulse is far steeper than the trailing edge, and this effect is particularly noticeable for the x rays with $\hbar\omega \sim 10$ keV (Fig. 4). It is thus natural to suggest that after a rapid contraction in the course of the pinch an equilibrium is established in the plasma of the vacuum spark, and the subsequent evolution of the plasma is governed by the slow changes in the equilibrium values of the various properties.

3. THEORETICAL CONCEPTS REGARDING MICROPINCHES

Our analysis of the micropinch is based on a study of the equilibrium of the plasma with the current. By taking this approach we can find a consistent description of the variety of phenomena which accompany the pinch in the vacuum diode, and at the same time we can at least partially bridge the gaps which arise because of

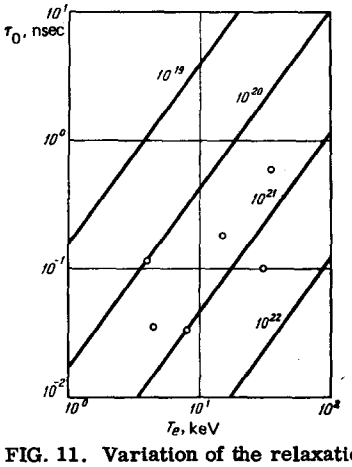

FIG. 11. Variation of the relaxation time τ_0 due to Coulomb collisions with the temperature T_e for fixed values of the density n_e (the curve labels). The circles show the states of the plasma according to the experiments of Refs. 31, 32, 34, 35, 37, and 41.

attempts to single out various individual properties of the micropinch for explanation.

The stage of the slow decay of the emission burst from the micropinch can be described on the basis of the equilibrium theory of Ref. 22 and the theory of collisionless emission.[24] The theoretical conclusions agree with experiment and make it possible to reconstruct the time evolution of the decay of the electron temperature during the radiative cooling.

An accurate quantitative description of the initial stage of the rapid contraction of the micropinch requires a theory for the evolution of the plasma in the course of a pinch—a theory which is not available. The question becomes even more complicated when we try to take into account the effect on the contraction of the synchrotron radiation of the electrons in the magnetic field produced by the strong current. To a large extent, the difficulties stem from the fact that the micropinch is optically dense for the synchrotron radiation of the plasma, but at the same time (during the contraction stage) it is very nonequilibrium formation. Under these conditions, the radiation transport is not simply radiative heat transfer, as it is in the physics of stellar atmospheres.[56] Because of the large number of photons (the radiation is trapped) and the nonequilibrium energy distribution of the electrons during the fast contraction stage we must take into account the induced synchrotron radiation. Below we shall estimate the intensity of this radiation in order of magnitude.

The theory for the micropinch is far from complete at present. Questions which remain to be dealt with are neutron emission and the collective acceleration of charged particles.

(a) Plasma equilibrium in the magnetic field of the current

The equilibrium of a self-contracting plasma in the strong magnetic field produced by a current was first studied by Bennett.[57] There is a detailed bibliography on the question in the reviews in Refs. 58–61.

Since the relaxation time τ_0 is short in comparison with the duration of the emission burst, it can be assumed that an equilibrium is established separately in the electron subsystem and the ion subsystem. A thermal equilibrium between these subsystems is not attained because of both the large mass difference and the drift caused by the external field applied to the diode. In this formulation of the problem there is no ambiguity in the choice of a distribution function. In Refs. 22 and 62 there is a detailed analysis of all possible cylindrically symmetric configurations of a plasma consisting of ions which are at rest on the whole and electrons which carry the current.

The equilibrium state of a cylindrically symmetric plasma with a current is characterized by the five properties

$$N_e,\ N_i,\ T_\perp,\ T_i,\ \beta. \tag{1}$$

Here N_e and N_i are the numbers of electrons and ions per unit length of the spark, T_e and T_i are the electron and ion temperatures, $T_\perp = T_e\sqrt{1-\beta^2}$ is the effective electron temperature in the transverse direction, $\beta = v_0/c$, and v_0 is the electron drift velocity with respect to the ions, which is related to the total current I by $I = eN_e v_0$. Since the electrons as a system are in motion with respect to the ions, the two systems are attracted to each other as parallel currents. This attraction occurs in addition to the electrostatic interaction with the space charge. If the numbers of particles per unit length of the discharge, N_e and N_i, satisfy the inequalities $N_e > ZN_i > N_e(1-\beta^2)$, then both the electrons and the ions are subjected to long-range forces, exerted by the other charges, which attract them toward the axis. The potentials for these forces are different for the electrons (U_e) and the ions (U_i). These potentials are quadratic functions of the radius near the axis, while far from the axis they increase logarithmically with increasing r:

$$U_e = 2\varepsilon_e \ln r,\ U_i = 2\varepsilon_i \ln r,\ r \to \infty.$$

Here $\varepsilon_e = e^2(ZN_i - (1-\beta^2)N_e)$ and $\varepsilon_i = Ze^2(N_e - ZN_i)$ are the energies associated with the attraction of the electron and the ion by the other charges in the collective interaction field. In this field, the equilibrium density distributions for the electrons and ions fall off in a powerlaw manner with increasing r: $n_e \sim r^{-2K_e}, n_i \sim r^{-2K_i}$, in the limit $r \to \infty$, where $K_i = \varepsilon_i/T_i$ and $K_e = \varepsilon_e/T$. The conditions that the numbers of particles, N_e and N_i, must be finite, which are equivalent to the conditions that the current and charge of the spark must be finite, are[22]

$$K_e > 1,\ K_i > 1, \tag{2}$$

so that the energy of the attraction between the charges must exceed the energy associated with the thermal dispersal of these charges in the transverse direction. Conditions (2) are essentially unrelated to the existence of an equilibrium in the plasma; they simply follow from the convergence of the normalization integrals $N_\alpha = 2\pi\int_0^\infty n_\alpha(r) r dr$ at the upper limit.

The properties in (1) are not independent if the plasma is at equilibrium in the approximation of the classical statistics of ideal gases. These properties must be chosen to satisfy a balance equation involving the energy associated with the magnetic compression, $\frac{1}{2}e^2N_e^2\beta^2$, that associated with electrostatic repulsion, $(\frac{1}{2})e^2(N_e - ZN_i)^2$, and the kinetic energy of the charges, $N_iT_i + N_eT_\perp$, per unit length of the spark[63]:

$$N_iT_i + N_eT_\perp + \tfrac{1}{2}e^2(N_e - ZN_i)^2 = \tfrac{1}{2}e^2N_e^2\beta^2. \tag{3}$$

For an electrically neutral plasma, with $ZN_i = N_e \equiv N$, Eq. (3) reduces to the Bennett equilibrium condition[57]: $I^2 = 2c^2N(T_\perp + T_i)$.

The radial profiles of the charge densities of the potentials U_e and U_i have only been determined numerically for the general case.[62,64] Some illustrative profiles $n_\alpha(r)$ and $U_\alpha(r)$ ($\alpha = i, e$) are shown in Fig. 12 for certain values of the parameters.

A distinguishing property of the equations governing the structure of the equilibrium, cylindrically symmetric discharge channel in the approximation of the classical statistics of ideal gases is gauge invariance.[22]

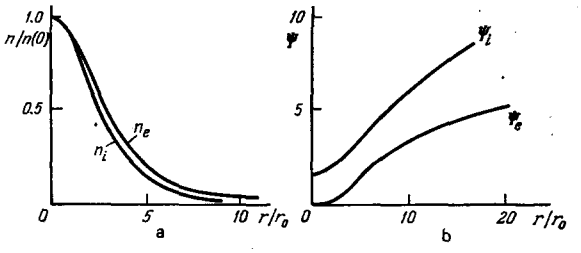

FIG. 12. Radial profiles of the charge density (a) and the potential (b) found through a numerical integration for the following parameter values: $\beta=0.98$, $K_e=1.01$, $K_i=4.28$ ($T_i/T_1=5$).

The equilibrium profiles of the potential $U_\alpha(\alpha=i,e)$ depend on r through the combination r/r_0, where r_0 is an arbitrary scale parameter. The physical reason for the gauge invariance is that, as the cross section of the discharge channel changes, the energies associated with the magnetic contraction, the electrostatic repulsion, and the thermal expansion in the radial direction all vary with the radius in the same way. Where gauge invariance holds, the conditions for an equilibrium of forces do not determine the micropinch radius.

In order to determine the micropinch radius and also the temperature of the charges–these properties determine the plasma configuration at equilibrium–it is necessary to study the energy transport equation. The evolution of a plasma with Joule heating and with energy removal by radiation is studied below, in Subsection d1 of Chapter 3. At a current of the order of 1 kA, however, the energetically equilibrium value of the pinch radius may be so small that it is actually not reached, because electron degeneracy comes into play. When a plasma is compressed to a degenerate state, the pressure of the electron Fermi gas increases more rapidly with decreasing radius of the current channel than does the pressure of an ideal gas or the magnetic pressure. The equations governing the mechanical equilibrium of a plasma in a collective interaction field with electron degeneracy are no longer gauge-invariant.[22] Consequently, when a plasma is compressed to the point of electron degeneracy, the radius of the current channel is determined directly from the condition for mechanical equilibrium.

Electron degeneracy comes into play at a density $n_e \sim n_{e\,\mathrm{deg}}=(mT_e/\hbar^2)^{3/2}$. The equilibrium radius r_0 of a plasma which has contracted to the point of electron degeneracy varies over a broad range, depending on the discharge current (or on N_e). To estimate this radius it is convenient to work from the condition $n_{e\,\mathrm{deg}}\pi r_0^2 \approx N_e$. We find

$$r_0 \sim N_e^{1/2}\hbar^{3/2}(mT_e)^{-3/4}. \tag{4}$$

In micropinch contraction to a degenerate state, the typical electron density is $n_e \sim 10^{30}$ cm^{-3}, and the typical equilibrium radius is $r_0 \sim 10^{-8}$ cm.

The equilibrium of a pinch contracted to the point of electron degeneracy was studied in Refs. 22, 64, and 65. Since the ion mass is much larger than the electron mass, the ions can be treated as an ideal gas obeying Boltzmann statistics. The calculation of the structure of the spark channel with a Fermi electron energy distribution is reminiscent of the calculations of the structure of a many-electron atom by the Thomas–Fermi method[66] and the calculation of the structure of a nonrelativistic cold star.[67]

In contrast with atoms, ions are not localized at the center as in a nucleus; their radial profile is also determined from the equilibrium conditions. Generally speaking, the size of the volume occupied by the electrons is of the same order of magnitude as that of the volume occupied by the ions. Furthermore, the electrons are drifting along the discharge channel with respect to the ions. The state of maximum compression can be thought of as a "linear atom" consisting of ions which are at rest on the whole and drifting electrons. Different electrons transverse the micropinch region at different times, while the radial profile of the electron density is approximately a steadystate profile. If the micropinch contracts to the point of electron degeneracy, then we would have in the micropinch region a laboratory case of condensed matter at high temperatures, i. e., matter in a state similar to that in the interior of stars.[68]

At temperatures $T_e \gg E_a=27.2$ eV, which are of interest in connection with the fusion problem, the radius of the micropinch region increases in accordance with (4) as the electrons cool off.

The energy of the collective magnetic contraction per atom is given in order of magnitude by

$$\varepsilon_{\mathrm{coll}} = Z\varepsilon_e + \varepsilon_i = Ze^2N_e\beta^2. \tag{5}$$

Since the ions are at rest on the whole, the potential (U_i) of the forces acting on the ions is equal to the scalar potential φ of the electromagnetic field of the collective interaction. Assuming $U_i \sim 2\varepsilon_i \ln(r/r_0) \sim \varepsilon_{\mathrm{coll}}$, we find the following estimate of the electric field E_r in the micropinch region, using (4) and (5):

$$E_r \sim \frac{\varepsilon_{\mathrm{coll}}}{Zer_0} \sim \frac{m^2c^{5/2}}{\hbar^{3/2}}\beta^2\left(\frac{e^2N_e}{mc^2}\right)^{1/2}\left(\frac{T_e}{mc^2}\right)^{3/4} \sim 10^{15}\beta^2\left(\frac{e^2N_e}{mc^2}\right)^{1/2}\left(\frac{T_e}{mc^2}\right)^{3/4} \text{ V/cm}.$$

At a current of the order of 100 kA, this field could explain the observed spectral-line broadening in the micropinch plasma[37,41,46] as a consequence of the Stark effect. It would thus be possible to explain the observed increase in the line width with increasing value of n, the principal quantum number.[46]

(b) Motion of the charges in the micropinch region

Let us examine the motion of the electrons in the cylindrically symmetric plasma of a micropinch. The motion of the individual charges is governed by collective-interaction forces. The transverse motion of the charges is bounded, and the energy spectrum is discrete. However, under the condition

$$I \gg \frac{mc^3}{e}\left(\frac{e^2}{\hbar c}\right)^{1/2}\left(\frac{T_e}{mc^2}\right)^{3/4}$$

even if the plasma is compressed to the point of electron degeneracy, the level spacing is small in comparison with the characteristic values of the energy, so

that the motion is semiclassical, and classical mechanics can be used.

Gratreau[69] has analyzed the trajectories of the individual particles in a plasma with a high current for the case of a Bennett equilibrium. We shall restrict the present discussion to the most important limiting cases of weak and strong currents.

In the weak-current limit,

$$I \ll \frac{mc^3}{e} = 17 \text{ kA}, \quad \beta \sim 1, \tag{6}$$

the electron Larmor radius in the magnetic field of the current is large in comparison with the plasma radius. In this case the electron motion reduces to transverse oscillations in the field $U_e(r)$ and an equilibrium motion along the axis.

In the opposite limit, of a strong current,

$$I \gg \frac{mc^3 v_T}{e}, \quad v_T = \sqrt{\frac{2T_e}{m}}, \tag{7}$$

the electron Larmor radius is small in comparison with the transverse plasma dimensions r_0. In this case, with $T_e \ll mc^2$ and $\beta \ll 1$, each individual electron moves uniformly along the azimuthal direction (along the magnetic field), executes small oscillations in the direction perpendicular to the magnetic field, and drifts along the discharge axis under the influence of the mutually perpendicular electric and magnetic fields of the collective interaction. The net electron drift of all the electrons produces the total current in the plasma.

The ratio of the energy of the radial oscillations to the Larmor frequency, $mv_{r_0}^2/2\Omega_0$, is an adiabatic invariant, as is the angular momentum $M = rp_\varphi$. It can be shown that at a constant current I, with slow variations in the plasma radius r_0, for example, along the discharge axis (z), the radial and drift velocities are described by

$$v_{r_0} \sim r_0^{-1/2}, \quad v_0 \sim r_i^{-2}, \quad \beta \ll 1. \tag{8}$$

In the case of a pronounced contraction of the discharge channel, the electrons may be accelerated to relativistic velocities; then the relations in (8) would change. It is important to note, however, that the electron drift at the "bottleneck" is intensified to a far greater degree than the thermal velocity spread. This means that in the region of maximum compression the plasma electrons constitute a beam (a relativistic beam if the contraction is sufficiently pronounced), while outside this region the electrons again constitute an ordinary plasma with a current. The highly magnetized electrons constitute a sort of incompressible fluid, so that the second relation in (8) is equivalent to constancy of the product of the flow velocity and the cross-sectional area, which follows from the continuity equation. The emission of x rays in the micropinch and the absence of emission from the anode surface reported in Ref. 31 can be explained on the basis that as the current channel expands from the micropinch region toward the anode the electrons rapidly lose directed-motion energy, in accordance with (8), and they are essentially cold when they reach the anode.

Experimentally, the appearance of a micropinch during the contraction of the discharge channel is accompanied by a sharp decrease in the current, by about 30% of its value at the time of the drop. Rapid changes in the current induce strong electric fields in the plasma, which in turn tend to prevent changes in the current. These fields may also be responsible for the acceleration of charges.[70] Fukai and Clothiaux[71] have analyzed the mechanism for electron acceleration upon a sudden current cutoff in connection with the vacuum spark. They showed that if the current before cutoff is 100 kA the maximum energy to which iron ions can be accelerated is 40 keV, while electrons can be accelerated to 20 MeV. The mechanisms for charge acceleration with an adiabatic change in the channel radius and with a current cutoff corresponds to the opposite limiting cases of slow and fast changes in the plasma configuration. Curiously, the contraction of the discharge channel is accompanied in both cases by an acceleration of charges in the current direction.

(c) Collisionless emission

The formation of the micropinch and its subsequent evolution are closely related to the removal of energy by radiation. The primary emission mechanism in a plasma is usually assumed to be the bremsstrahlung of electrons in binary collisions with ions. The emission caused by Coulomb collisions of the charges plays the leading role in a homogeneous plasma without electromagnetic fields. In the case of a strong magnetic compression of the current, the plasma configuration is governed by the electromagnetic forces of a collective interaction. The charges subjected to these forces are accelerated and radiate. The radiation is bremsstrahlung in the collective interaction field. Since this emission is not related to binary collisions of charges, it is naturally called "collisionless." To compare this collisionless emission with the emission which occurs in Coulomb collisions it suffices to estimate the acceleration experienced by the charges in the two cases. In a hot plasma, with a mean free path l comparable to r_0 (the characteristic dimension for a change in the density), the acceleration in the case of a bounded motion in the radial direction is greater than the acceleration caused by binary collisions. The collisionless emission becomes predominant at $l \gtrsim r_0$, since the relative change in the velocity is small in the case of Coulomb collisions. Budker[72] pointed out the need to consider collisionless emission at high currents because of the increased importance of the collective interaction.

Calculations were carried out in Ref. 24 for the collisionless emission of a cylindrically symmetric plasma in the simple case in which the photons emitted by the charges escape from the plasma without any significant absorption by other charges. The corresponding condition is $\delta \gg r_0$ ($\delta \sim c/\omega_0$ is the depth to which a field at a frequency $\omega \leq \omega_0$, where ω_0 is the plasma frequency, penetrates into the plasma), and in the case $\beta \sim 1$ it reduces to the weak-current condition in (6). The intensity of the collisionless emission in the case of a weak current is proportional to the square of the temperature and inversely proportional to the square of the plasma radius.[24] During the plasma contraction and

heating, the intensity of the collisionless emission increases more rapidly than does that of the emission which occurs in Coulomb collisions. In the weak-current limit, the collisionless emission is associated with the radial oscillations of the electrons. The angular distribution of this current is described by

$$\frac{dJ}{d\Omega} \sim 1 - \frac{1}{2}\sin^2\theta, \quad \beta \ll 1, \tag{9}$$

where θ is the angle between the propagation direction of the radiation and the current direction. The spectrum of the collisionless emission in the weak-current limit, (6), is governed by the circumstance that each electron emits at the frequency $\omega \sim v_T/r_0$, which is the frequency of its transverse oscillations. At high frequencies, $\omega \gg v_T/r_0$, the intensity of the emission for an arbitrary $\hbar\omega/T_\perp$ is given by[24]

$$\frac{dJ}{dz\,d\omega\,d\Omega} = A\sqrt{\ln\frac{\omega r_0}{v_T}}\left\{\exp\left[\frac{\hbar\omega(1-\beta\cos\theta)}{T_\perp}\right]-1\right\}^{-1}, \quad \omega \gg v_T/r_0. \tag{10}$$

The factor A is independent of the frequency and temperature. We do not need to know its exact value, since we have not absolute measurements of the emission intensity for comparison.

In the strong-current limit, (7), the electron Larmor radius in the magnetic field of the current is small in comparison with the plasma radius. The magnetic field of the current varies only slightly over the electron orbit. In case (7), the collisionless emission reduces to the synchrotron radiation of electrons in the magnetic field of the current. Vikhrev and Korzhavin[73] have calculated the intensity of the equilibrium synchrotron radiation from an inhomogeneous plasma with a strong current in connection with the plasma focus. Since the emission is important in electromagnetic compression, we will give the necessary estimates of the synchrotron radiation of a cylindrically symmetric plasma. The estimates below do not take the exact plasma configuration into account, so that they are correct only in order of magnitude.

The total intensity of the synchrotron radiation of an electron which is moving at a velocity v across the magnetic field H is (Ref. 74, §74)

$$I = \frac{2e^4H^2v^2\gamma^2}{3m^2c^5} = \frac{2}{3}\frac{e^2}{c^3}\Omega^2v^2\gamma^2.$$

In the high-current case, (7), the depth to which the field penetrates into the plasma, δ, is small in comparison with r_0: $\delta/r_0 \sim \sqrt{mc^2/e^2N_e} \sim \sqrt{mc^2v_0/eI} \ll 1$. Under these conditions, the only photons which escape from the plasma are those which are emitted within a short distance of order δ from the surface. As $\tilde{N}$, the effective number of radiators, we should thus adopt $\tilde{N} \sim N_e\delta/r_0 \sim N_e\sqrt{mc^2/e^2N_e}$, where N_e is the number of electrons per unit length of the discharge. Noting that $\Omega \sim e^2N\beta/mcr_0$, and assuming $v^2 \sim T_e/m$, we find the following estimate of the intensity of the spontaneous synchrotron radiation:

$$\frac{dJ^{sp}}{dz} \sim \left(\frac{e^2Ne}{mc^2}\right)^{5/2}\frac{T_e\beta^2c}{r_0^2}.$$

The electrons in the plasma also continuously emit and absorb photons. Essentially none of the photons escape from the plasma, so that a certain steady-state number of photons is built up in the discharge. If the plasma were at thermal equilibrium, blackbody radiation with a spectral density $e_0(\omega)$ would be trapped in it (Ref. 75 §63), and the radiative energy flux across a unit area of any surface in the plasma in each direction would be $dI \sim ce_0(\omega)d\omega$. If there is no thermal equilibrium in the plasma, and there is a population inversion for the higherlying energy levels, then the photon flux reaching the radiating surface layer will cause an induced emission. The probability for this emission, w^{in}, is related to w^{sp}, the probability for spontaneous emission, by (Ref. 76, §44)

$$w^{in} = w^{sp}\frac{\pi^2c^3}{\hbar\omega^3}\frac{dI}{d\omega}.$$

If the photon flux density is assumed to be on the order of the blackbody flux density, $(\pi^2c^2/\hbar\omega^3)\,dI/d\omega \sim T/\hbar\omega$, $\hbar\omega \ll T$, we would have the following estimate of the intensity of the induced synchrotron radiation of a cylindrically symmetric nonequilibrium plasma in the high-current limit ($\omega \sim \Omega$):

$$\frac{dJ^{in}}{dz} \sim \left(\frac{e^2N_e}{mc^2}\right)^{3/2}\frac{T^2\beta}{\hbar r_0}. \tag{11}$$

If $\beta \lesssim 1$, the synchrotron intensity reaches a maximum at the gyrofrequency, $\omega \sim \Omega$, and in the ultrarelativistic case this maximum shifts to a higher frequency (Ref. 74, §74): $\omega \sim \Omega\gamma^2$, $\gamma = (1-\beta^2)^{-1/2} \gg 1$. Estimate (4) can be used for the plasma radius in a state of electron degeneracy. Assuming $H \sim I/cr_0$, we find the characteristic energy of the emitted photons to be

$$\hbar\omega \sim mc^2(\alpha\beta)^{1/2}\gamma^2\left(\frac{T_e}{mc^2}\right)^{3/4}\left(\frac{eI}{mc^3}\right)^{1/2}, \quad e^2N_e \gg mc^2. \tag{12}$$

For temperatures of the order of hundreds of keV and currents of the order of 100 kA, this characteristic energy corresponds to the hard x-ray region. The emission of hard photons in the vacuum spark of a high-current diode can thus be explained as the synchrotron radiation of electrons in transitions betweed Landau levels in the strong azimuthal magnetic field of the current, in the sate of maximum contraction and heating of the micropinch plasma.[24] In other words, the hard photons are emitted in transitions of electrons between quantum levels of the linear atom. The distance between adjacent levels, $\Delta\varepsilon = \hbar\Omega$ in (12), is greatest in the stage of the maximum contraction and heating.

The possible mechanisms for the emission of hard photons in a vacuum spark, which were studied by Fukai and Clothiaux[71], involve the presence of electrons accelerated to the necessary energy by the induced electric field which arises in the plasma during the rapid current changes. Fukai and Clothiaux studied the emission of hard photons in collisions of accelerated electrons with an anode surface, and they suggested a possible mechanism for the emission of photons as the accelerated electrons move in a collective interaction field. The mechanism described above, according to which hard photons are emitted in electron transitions between Landau levels, is essentially a specific example of the emission of a photon by an electron in a collective interaction field.

As a possible cause of the sharp current drop, Fukai and Clothiaux[71] studied the anomalous resistance of a plasma which can become turbulent because of electrostatic instabilities. The question of the stability of an

equilibrium plasma during the pinch effect was formulated in its most general form in the review by Buneman.[59] The problem of the stability of pinch systems is a complicated mathematical problem, however, and it is sensitive to the particular experimental conditions; the net result is that no general solution exists. With regard to the dense plasma of a micropinch, the stability question remains open, to the best of our knowledge. The related problem of the resistive firehose instability of a beam with a Bennett profile in the collisionless limit was studied theoretically by Lee[77] and experimentally by Lauer *et al.*[78]

The mechanism for the increase in the drift velocity during an adiabatic slow contraction of a current channel, (8), can be used to explain electron acceleration without resorting to the mechanism of acceleration in the induced field, which is based on the assumption that instabilities may occur in the plasma in the current channel.

Recent experimental evidence shows that at the time of the current cutoff it is the micropinch region, rather than the electrode surface, which is the source of most of the x radiation.[31,40]

The angular distribution of the synchrotron radiation differs from the distribution in (9), for the radiation caused by radial oscillations in the weak-current limit, (6). Since the magnetic field varies only slightly over an electron orbit in the strong-current case, (7), we can use the equation (Ref. 74, §74) $dI/d\Omega \sim 2-\cos^2\vartheta$, $\beta \ll 1$. Here ϑ is the angle between the direction in which the radiation is propagating and the plane running perpendicular to the vector H. This angle can be expressed in terms of θ, which is the angle between the radiation direction and the current, and the azimuthal angle φ: $\sin\vartheta = \sin\theta\sin\varphi$. After an integration over φ, in the nonrelativistic limit, we find

$$\frac{dJ}{d\Omega} \sim 1+\frac{1}{2}\sin^2\theta, \quad \beta \ll 1. \tag{13}$$

The angular distribution of the radiation makes it possible to distinguish between the emission mechanisms in the opposite limiting cases of weak and strong currents, (6) and (7), respectively. It can be assumed that the angular distribution found in Ref. 36 for the microwave emission of a plasma focus (Fig. 3a) at the beginning of the burst corresponds to the mechanism of electron synchrotron radiation. The curve in Fig. 3a is plotted from Eq. (13), while the points are experimental.[36] The angular distribution in the final stage (Fig. 3b) apparently corresponds to the emission associated with the radial oscillations with a weak current. The solid curve in Fig. 3b is plotted from Eq. (9), while the points are experimental.[36] Since the current in this case is measured in hundreds of kiloamperes and is not weak, these results may imply that the current in the final stage of the burst is not distributed uniformly over the plasma but instead has a complicated spatial structure. The emission is most intense from the regions of pronounced plasma contraction; the relative importance of these regions in the current flow may be slight. The possibility that the current flows in distinct channels is pointed out in Refs. 55 and 79. The conclusion that the current flows through distinct channels corresponds to the inhomogeneity of the x-ray emission[46,54,55] and the pronounced angular anisotropy of this emission[40] which have been observed experimentally.

(d) Evolution of the vacuum spark

No quantitative description is available for the evolution of a micropinch in a vacuum diode. A qualitative picture and order-of-magnitude estimates can be constructed from the theory of the equilibrium and of collisionless emission.

The logarithmic long-range increase in the potentials U_e and U_i is actually not a consequence of the equilibrium in the plasma; it is caused solely by the cylindrical geometry and the conditions that the current and charge in the plasma must be finite. This statement is equally true of the inequalities (2), which restrict the range of parameters within which both the ions and the electrons are attracted to the axis by the forces exerted by the other charges. These forces are capable of restraining the transverse dispersal of the charges. In the absence of an equilibrium, the term "temperature" should be understood as the average kinetic energy of the corresponding charges.

1) Dynamics of the contraction and radiative collapse

The electrons striking the anode during the discharge damage the anode surface. Near the anode, positive ions are formed through the ionization of atoms by the electrons which are carrying the current. The electrons which are produced in the course of the ionization are repelled by the electrons which are carrying the current. The repelled electrons either reach an equilibrium with the electron beam or move away in the radial direction. The ions, on the other hand, are attracted, and they accumulate near the discharge axis. When a number of ions enter the region defined by (2), both the ions and the electrons are subjected to forces from the other charges which attract them to the axis. These forces are capable of restraining the radial dispersal of the charges. These forces cause a collapse of the plasma, and a pinch occurs. The self-contraction conditions in (2) may be arranged anywhere in the discharge gap, not necessarily beside the anode.

The Bennett equilibrium in (3), at a fixed current of the order of 100 kA, can occur only at a very high temperature, of the order of hundreds of keV. Thus the pressure of the magnetic field produced by the current is not balanced in a cold plasma. This state is hydrodynamically unstable, and the collective interaction forces compress the plasma to the axis. In the course of this compression, the electron temperature rises. The behavior of this temperature is governed by the heat-transfer equation

$$T_e\frac{dS}{dt} = \frac{dQ}{dz} - \frac{dJ}{dz}, \tag{14}$$

where $S = N_e \ln r_0^2 T_e^{3/2}$ is that part of the electron entropy per unit length of the spark (in the approximation of the classical statistics of ideal gases) which depends on r_0 and T_e.

Equation (14), along with the equations of motion,

describes the dynamics of the plasma contraction and heating. In the first part of the contraction, both emission and ohmic heating can be ignored, and it can be assumed that the right side of Eq. (14) is zero. This initial stage consists of the adiabatic contraction and heating of the plasma, culminating in the attainment of a Bennett equilibrium state, (3). During pronounced contraction and heating of a plasma in a state near a mechanical equilibrium, the evolution depends on the relation between the energy flows into and out of the plasma. We will assume that the primary mechanism by which energy is transferred to the electrons is Joule heating,

$$\frac{dQ}{dz}=\left(\frac{dQ}{dz}\right)_J \sim \frac{Ze^4 m^{1/2}\Lambda N_e^2\beta^2 c^2}{T_e^{3/2} r_0^2}, \qquad (15)$$

while the primary mechanism by which energy is lost is radiation.

The energy balance between ohmic heating and the radiative energy loss in pinches has been studied in Refs. 80–84. The primary emission mechanism is usually assumed to be the bremsstrahlung caused by binary collisions of electrons with ions. The corresponding intensity per unit length of the spark, dJ/dz, varies with the radius of the current channel (r_0) in the same way as the Joule heating, given in (15). In the case of a Bennett equilibrium, (3), the energy carried away by bremsstrahlung becomes equal to the Joule heat at a certain fixed current I_{PB}, which is independent of the plasma density, the temperature, and the radius.[80-83] This Pease–Braginskii current is of the order of 10^6 A. At a current $I<I_{PB}$, the plasma expands, while with $I>I_{PB}$ it undergoes an unrestricted contraction toward the channel axis (it collapses).

The use of the equations for the emission intensity in the case of Coulomb collisions rests on two assumptions: First, it is assumed that the plasma state changes only slowly, and that both a mechanical equilibrium and a thermal equilibrium are established at each instant. Under this assumption it is possible to use the standard equations for the emission intensity of an equilibrium plasma. Second, it is assumed that the intensity of the emission due to Coulomb collisions is higher than that of the collisionless emission. Neither of these assumptions holds in the stage of the micropinch contraction. As the temperature is raised, the mean free path of the electrons with respect to Coulomb collisions increases rapidly, and in the stage in which the emission must be taken into account this mean free path becomes larger than the radius of the spark channel. As shown in Subsection 3c, collisionless emission is predominant in this case, and the emission caused by binary collisions is of secondary importance. In the strong-current case in which we are interested, (7), the primary emission mechanism in the contraction stage should be identified as the magnetobremsstrahlung of the electrons in the magnetic field produced by the current.

During the collapse stage, the state of the plasma changes so rapidly that a thermal equilibrium of the electrons cannot be established. The nonequilibrium heating of the electrons results in a population inversion in the energy levels. If there is no equilibrium, the induced emission processes are not balanced by induced absorption. In this case, we should use the estimate in (11), for the intensity of the induced synchrotron radiation of the electrons, as the emission intensity dJ/dz in Eq. (14).

At temperatures of the order of the contraction energy in (5), the Joule heating becomes comparable to the emission intensity in (11) at the micropinch radius

$$r_0 \sim \frac{\hbar}{mc}\frac{Z\Lambda}{\beta^3}\left(\frac{mc^2}{eI}\right)^3. \qquad (16)$$

At smaller radii, the Joule heating is faster than the radiative energy loss; there is a net energy transfer to the electrons, and the plasma expands. If, on the other hand, r_0 is larger than the value in (16), energy is carried off by the radiation faster than it is provided by the Joulean heating. The energy difference is made up by the internal energy of the plasma which is released during the contraction. The contraction continues until the plasma radius reaches the value in (16). Relation (16) thus gives us, in order of magnitude, the energetically equilibrium radius of a plasma which is in the state of mechanical equilibrium described by (3).

As the current increases, the equilibrium radius in (16) falls off rapidly, and at a certain critical current I_{cr} it falls below the radius in (4), which corresponds to a plasma which has been compressed to the point of electron degeneracy. In other words, at a current above the critical value,

$$I>I_{cr} \sim \frac{mc^3}{e}\left(\frac{\alpha Z^2\Lambda^2}{\beta^8}\right)^{2/11} \qquad (17)$$

($\alpha=e^2/\hbar c=1/137$ is the fine structure constant), the plasma reaches an equilibrium in which the magnetic pressure is balanced by the pressure of the electron Fermi gas, as the result of the contraction and heating in the initial stage and the contraction due to the radiative energy loss (radiative collapse) in the heated state. At the point of maximum contraction, the micropinch is a sort of linear atom in which the ions as a whole are at rest, while the electron states are filled by drifting electrons which are carrying a current. The observed emission burst from the micropinch is naturally associated with the emission by electrons in transitions between quantum levels in the course of populating the low-lying states of the linear atom.

The critical current in (17), at which, during the rapid contraction, the pinch may reach a condensed state of a linear atom, is roughly two orders of magnitude lower than the Pease–Braginskii current. The critical current in (17) is relatively low because the energy removal by synchrotron radiation is relatively fast (in comparison with Coulomb collisions), and this synchrotron radiation is of an induced nature in the case of a rapid contraction.

In the initial stage of the pinch, the net magnetic-compression energy per atom, (5), is of the order of $Ze^2N_e\beta^2$, so that the contraction velocity can be estimated to be $v_r \sim (Ze^2N_e\beta^2/M)^{1/2}$, where M is the ion mass. In the heated state, in the stage of the radiative collapse, the magnetic pressure is balanced by the temperature, and the contraction rate is governed by

the rate at which energy is removed by radiation: $v_r \sim c\alpha\beta^{1/2}(eI/mc^3)^{3/2}$. In both cases, the contraction velocity is of the order of 10^8 cm/sec for a current of the order of 100 kA.

Such a high velocity of the radial contraction may mean that actually the intial stage of the contraction and heating during the pinch process may not only be a nonequilibrium stage but may also be accompanied by the onset of MHD flows, which are generally not cylindrically symmetric. The anomalous resistance which arises in the initial stage of the contraction due to the onset of turbulent flow may explain the drops in the current, which have relative magnitudes[31] of up to 30%. If the current does not fall below the critical value in (17), the plasma contraction continues, and as a result of the radiative collapse the plasma may reach an equilibrium maintained by electron degeneracy.

In the course of the radiative contraction, the scale time for the relaxation due to Coulomb collisions, τ_0, decreases markedly, and in the degenerate state this time becomes

$$\tau_{0\,\mathrm{deg}} \sim \frac{m^{1/2}T_e^{3/2}}{e^4 n_{e\,\mathrm{deg}}\Lambda} \sim \frac{\hbar^3}{e^4 m\Lambda} \sim 10^{-16}\ \mathrm{sec}\ .$$

This result means that in the stage of radiative collapse the turbulent fluctuations are damped, and the plasma rapidly reaches an equilibrium.

In describing the course of the contraction we have ignored the energy exchange between electrons and ions, the release of fusion energy, and several other processes, on the basis that in the absence of accurate calculations of the induced synchrotron radiation the estimates found regarding the dynamics of the pinch effect would be at best correct in order of magnitude. An important conclusion is that the state of a linear atom can in principle be reached as the result of the radiative contraction of the plasma in the case of a strong current. The actual evolution of the micropinch region in a high-current diode, of course, depends on all the various processes which occur in the plasma.

The subsequent evolution of the plasma in the linear-atom state is apparently governed by radiative cooling. It follows from an analysis of the directional pattern of the microwave emission that the primary mechanism for energy removal in this stage should be considered to be the collisionless emission caused by the radial oscillations of the electrons. Working from the results of Ref. 24, we conclude that the intensity of the emission from the linear atom varies in accordance with $dJ/dz \sim T_e^{7/2}$. The electron energy of a unit length of the micropinch in the degenerate state is of order $E \sim \hbar^2 n_{e\,\mathrm{deg}}^{2/3} N_e/m \sim T_e N_e$ (Ref. 75, §57). If the change in the electron energy at a fixed value of N_e is caused by the radiation, and we can write $dE/dt = -dJ/dz$, then the electron temperature fall off over time in accordance with $T_e \sim t^{-2/5}$.

2) Characteristics of the emission and comparison with experiment

Substituting the time dependence of the temperature into (10), we find that the emission intensity in the high-frequency region falls off with time in accordance with the following law during the radiative cooling of the micropinch:

$$\frac{dJ}{dz\,d\Omega\,d\omega} \sim \exp(-bt^{2/5}), \quad \hbar\omega \gg T_e. \tag{18}$$

If it is assumed that by time t_0 the temperature has decayed to the value T_0, that is, $T_e(t) = T_0(t_0/t)^{2/5}$, then the constant b in 18) can be written

$$b = \frac{\hbar\omega}{T_0}(1-\beta\cos\theta)(1-\beta^2)^{-1/2}t_0^{-2/5}.$$

Comparing the decay law in (18) with the observations by Lee[32] (see Figs. 4 and 13a), we find the following for b and t_0: $t_0^{2/5}b = 4$, $t_0 = 20$ nsec. If it is assumed that in Ref. 32 the emission was observed in a direction perpendicular to the current ($\theta = \pi/2$), we can completely reconstruct the time evolution of the temperature $T_\perp$ during the course of the radiative cooling: $T_\perp(t) = 3(30/t)^{2/5}$ keV, where t is the time (in nanoseconds) which has elapsed since the beginning of the burst The results found for the temperature agree in order of magnitude with the experimental results (Table I).

The radiative cooling furnishes an explanation for the decrease in the duration of the emission with increasing photon energy. Figure 14 shows the temporal characteristics of the emission intensity for increasing photon energies. In agreement with the experimental observations by Lee[32] (Fig. 4), the duration of the emission falls off sharply with increasing photon energy. It is difficult to say anything definite about the quantitative agreement, however, for two reasons: First, Lee measured the emission intensity in arbitrary units, and these units are not necessarily the same for the different photon energies. Second, the duration of the emission of photons with energies above 60 keV is apparently shorter than the resolving time of the measurement apparatus.

The short duration of the emission of high-energy photons means that in the experiments we are actually

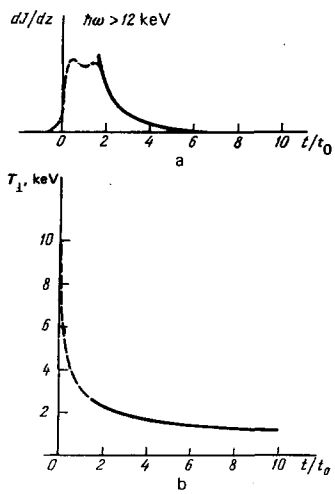

FIG. 13. a) Time evolution of the intensity of the x-ray emission of the micropinch [$\hbar\omega > 12$ keV. The dashed curve is experimental,[32] while the solid curve is constructed from Eq. (18)]; b) time evolution of the temperature $T_\perp$ constructed from Fig. 13a.

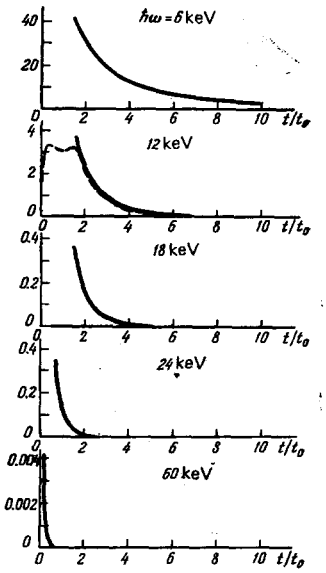

FIG. 14. Time evolution of the emission of x rays with various energies, according to (18). The dashed curve is experimental.[32]

not observing an instantaneous energy distribution of the photons; instead, we are observing average over the total duration of the burst. Integrating (18) over time, we find a power-law decay of the emission intensity with increasing photon energy:

$$\int_0^\infty \exp(-bt^{2/5})\,dt \sim b^{-2/5} \sim (\hbar\omega)^{-2/5}.$$

This behavior is shown by the dashed curve in Fig. 5. In this case, the experimental points of Ref. 32 correspond slightly better to an exponent of 4.5 (the solid curve in Fig. 5). The exponents reported by various experimentalists range from 2 to 5 (Refs. 32, 86, and 85).

4. CONCLUSION

Insofar as the fusion problem is concerned, the pinch in a high-current diode attracts interest because of the possibility of heating to fusion temperatures a strongly compressed plasma, whose expansion is prevented by collective interaction forces. The idea of using a self-contracting relativistic beam as a fusion reactor can be credited to Budker.[87] The primary objection to this idea is the pronounced radiative energy loss of the very hot electrons. Since the intensity of the emission by the electrons falls off in the course of the radiative cooling because of Fermi condensation of the electrons, it may be worthwhile to reexamine this objection.

It is natural to attempt to make use of the very nonequilibrium contraction in the initial stage of the pinch to pump highpower sources of induced synchrotron radiation over the spectral range from microwaves to hard x-rays.

Aside from its practical applications, the contraction of a plasma to the point of electron degeneracy in a high-current device is of much physical interest in itself, since this effect makes it possible in principle to produce in the laboratory condensed matter at high temperatures, i. e., matter in a state similar to that in the interior of stars.[68]

However, despite the fact that the experimental results on micropinches are consistent with, and in fact find a natural explanation in, the theory of the equilibrium and collisionless emission of a plasma heated to the point of electron degeneracy, there is still not enough evidence to prove definitely that linear atoms are present in a micropinch. Direct experiments are required to detect the strong electromagnetic fields and the high densities of matter in regions with dimensions measured in angstroms.

[1]L. Cohen, U. Feldman, M. Swartz, and J. H. Underwood, J. Opt. Soc. Am. 58, 843 (1968).
[2]S. V. Lebedev, S. L. Mandel'shtam, and G. M. Rodin, Zh. Eksp. Teor. Fiz. 37, 349 (1959) [Sov. Phys. JETP 10, 248 (1969)].
[3]A. A. Plyutto, K. N. Kevarlidze, and I. F. Kvartskhava, At. Energ. 3, 153 (1957).
[4]A. A. Plyutto, Zh. Eksp. Teor. Fiz. 39, 1589 (1960) [Sov. Phys. JETP 12, 1106 (1961)].
[5]S. K. Händel, Ark. Fys. 28, 303 (1964).
[6]I. Sundström, S. K. Händel, and J. E. Persson, Z. Phys. 200, 499 (1967).
[7]N. V. Filippov, T. I. Filippova, and V. P. Vinogradov, Nucl. Fusion, Part 2, Suppl., 577 (1962).
[8]J. W. Mather, Phys. Fluids 8, 366 (1965).
[9]R. W. Wood, Phys. Rev. 5, No. 1 (1897).
[10]R. A. Millikan and R. A. Sawyer, Phys. Rev. 12, 167 (1918); R. A. Millikan and J. S. Bowen, Phys. Rev. 23, No. 1 (1924).
[11]K. V. Suladze and A. A. Plyutto, Zh. Tekh. Fiz. 37, 72 (1967) [Sov. Phys. Tech. Phys. 12, 48 (1967)].
[12]A. A. Plyutto, P. E. Belensov, E. D. Korop, G. P. Mkheidze, V. N. Ryzhov, K. V. Suladze, and S. T. Temchin, Pis'ma Zh. Eksp. Teor. Fiz. 6, 540 (1967) [JETP Lett. 6, 61 (1967)].
[13]C. C. Lauritsen and R. A. Millikan, Phys. Rev. 31, 914 (1928); C. C. Lauritsen and R. D. Bennett, Phys. Rev. 32, 850 (1928).
[14]G. A. Mesyats and D. I. Proskurovskiĭ, Pis'ma Zh. Eksp. Teor. Fiz. 13, 7 (1971) [JETP Lett. 13, 4 (1971)].
[15]I. G. Kesaev, Katodnye protsessy élektricheskoĭ dugi (Cathode Processes in an Electric Arc), Nauka, Moscow, 1968.
[16]A. A. Lukashev, Zh. Tekh. Fiz. 31, 1262 (1961) [Sov. Phys. Tech. Phys. 6, 917 (1962)].
[17]T. H. Martin, IEEE Trans. Nucl. Sci. NS-16, No. 3, 59 (1969).
[18]G. N. Fursei and P. N. Vorontsov-Vel'yaminov, Zh. Tekh. Fiz. 37, 1870 (1967) [Sov. Phys. Tech. Phys. 12, 1370 (1968)].
[19]S. Frankel, V. Highland, T. Sloan, O. van Dyck, and W. Wales, Nucl. Instrum. Methods 14, 345 (1966).
[20]Yu. L. Stankevich and V. G. Kalinin, Dokl. Akad. Nauk SSSR 117, 72 (1967) [Sov. Phys. Dokl. 12, 1042 (1968)].
[21]L. V. Tarasova and L. N. Khudyakova, Zh. Tekh. Fiz. 39, 1530 (1969) [Sov. Phys. Tech. Phys. 14, 1148 (1970)].
[22]B. É. Meĭerovich and S. T. Sukhorukov, Zh. Eksp. Teor. Fiz. 68, 1783 (1975) [Sov. Phys. JETP 41, 895 (1975)].
[23]L. P. Pitaevskiĭ, Usp. Fiz. Nauk 90, 623 (1966) [Sov. Phys. Usp. 9, 888 (1967)].
[24]B. É. Meĭerovich, Zh. Eksp. Teor. Fiz. 71, 1045 (1976) [Sov. Phys. JETP 44, 546 (1976)]; 74, 86 (1978) [47, 44 (1978)].
[25]A. Englund and S. K. Händel, Z. Phys. 230, 193 (1970).
[26]T. G. Flynn, Proc. Phys. Soc., London, Sect. B 69, No. 439, 748 (1956).
[27]A. A. Plyutto, K. V. Suladze, E. D. Korop, and V. N. Ryzhkov, in: Proc. of the Fifth Intern. Symposium on Discharges and Electric Insulators in Vacuum, Poland, 1972, p. 145.
[28]G. I. Mkheidze, A. A. Plyutto, and E. D. Korop, Zh. Tekh.

Fiz. **41**, 952 (1971) [Sov. Phys. Tech. Phys. **16**, 749 (1971)].
[29]A. A. Plyutto, K. V. Suladze, S. M. Temchin, and E. D. Korop, At. Energ. **27**, No. 5 (1969).
[30]G. P. Mkheidze and E. D. Korop, Zh. Tekh. Fiz. **41**, 872 (1971) [Sov. Phys. Tech. Phys. **16**, 690 (1971)].
[31]W. A. Cilliers, R. U. Datla, and H. R. Griem, Phys. Rev. **A12**, 1408 (1975).
[32]T. N. Lee, Astrophys. J. **190**, 467 (1974).
[33]T. N. Lee and R. C. Elton, Phys. Rev. **A3**, 865 (1971).
[34]J. J. Turechek and H.-J. Kunze, Z. Phys. A **273**, 111.
[35]J. J. Turechek, Preprint No. 212P008, USA, 1972.
[36]G. Herziger, H. Krompholz, L. Michel, and K. Schönbach, Phys. Lett. **A64**, 51 (1977).
[37]É. Ya. Kononov, K. N. Koshelev, and Yu. V. Sidel'nikov, Fiz. Plazmy **3**, 663 (1977) [Sov. J. Plasma Phys. **3**, 375 (1977)].
[38]U. Feldman, S. Goldsmith, J. L. Schwob, and G. A. Doschek, Astrophys. J. **201**, 225 (1975).
[39]M. Klapisch, J. L. Schwob, B. S. Fraenkel, and J. Oreg, J. Opt. Soc. Am. **67**, 148 (1977).
[40]G. Herziger, H. Krompholz, L. Michel, and K. Schönbach, Phys. Lett. **A64**, 390 (1978).
[41]J. L. Schwob and B. S. Fraenkel, Phys. Lett. **A40**, 81, 83 (1972).
[42]É. Ya. Gol'ts, I. A. Zhitnik, É. Ya. Kononov, S. L. Mandel'shtam, and Yu. V. Sidel'nikov, Dokl. Akad. Nauk SSSR **220**, 560 (1975) [Sov. Phys. Dokl. **20**, 49 (1975)].
[43]P. G. Burkhalter, C. M. Dozier, and D. J. Nagel, Phys. Rev. **A15**, 700 (1977).
[44]W. H. Bostick, V. Nardi, W. Prior, and F. Rodriguez-Trelles, Bull. Am. Phys. Soc. Ser. II **17**, 1014 (1972).
[45]V. Nardi, in: Intern. Conference, Asty-Torina, Italy, November 5–6, 1974.
[46]R. U. Datla and H. R. Griem, Phys. Fluids **21**, 505 (1978).
[47]C. P. Bhalla, A. H. Gabriel, and L. P. Presnyakov, Mon. Not. R. Astron. Soc. **172**, 359 (1975).
[48]E. D. Korop and A. A. Plyutto, Zh. Tekh. Fiz. **41**, 1055 (1971) [Sov. Phys. Tech. Phys. **16**, 830 (1971)]; Izv. Vyssh. Uchebn. Zaved., Phys. No. 4, 131 (1973).
[49]E. D. Korop, Zh. Tekh. Fiz. **46**, 2187 (1976) [Sov. Phys. Tech. Phys. **21**, 1284 (1976)].
[50]N. V. Filippov and T. I. Filippova, Pis'ma Zh. Eksp. Teor. Fiz. **25**, 262 (1977) [JETP Lett. **25**, 241 (1977)].
[51]J. H. Lee *et al.*, Phys. Fluids **20**, 313 (1977).
[52]S. Lee and H. Conrads, Phys. Lett. **A57**, 233 (1976).
[53]V. V. Vikhrev, Fiz. Plazmy **3**, 981 (1977) [Sov. J. Plasma Phys. **3**, 539 (1977)].
[54]T. J. Welch and E. J. Clothiaux, J. Appl. Phys. **45**, 3825 (1974).
[55]W. H. Bostick, V. Nardi, and W. Prior, J. Plasma Phys. **8**, 7 (1972).
[56]S. Chandrasekhar, An Introduction to the Study of Stellar Structures, University of Chicago Press, Chicago, 1939.
[57]W. H. Bennett, Phys. Rev. **45**, 890 (1934).
[58]G. Benford and D. L. Book, in: Advances in Plasma Physics, Vol. 4, Wiley-Interscience, New York, 1971, p. 125.
[59]O. Buneman, in: Plasma Physics, McGraw–Hill, New York, 1961, Ch. 7, p. 203.
[60]B. N. Breĭzman and D. D. Ryutov, Preprint IYaF-119-74, Institute of Nuclear Physics, Novosibirsk, 1974.
[61]G. W. Wallis, K. Sauer, D. Sünder, S. E. Rosinskiĭ, A. A. Rukhadze, and V. G. Rukhlin, Usp. Fiz. Nauk **113**, 435 (1974) [Sov. Phys. Usp. **113**, 435 (1974)].
[62]V. N. Lyakhovitskiĭ, B. É. Meĭerovich, and S. T. Sukhorukov, Zh. Tekh. Fiz. **47**, 1719 (1977) [Sov. Phys. Tech. Phys. **22**, 996 (1977)].
[63]B. É. Meĭerovich and S. T. Sukhorukov, in: Élementarnye chastitsy (Elementary Particles), No. II, Atomizdat, Moscow, 1978, p. 14.
[64]S. T. Sukhorukov, Preprint ITÉF-171, Institute of Theoretical and Experimental Physics, Moscow, 1976.
[65]B. É. Meĭerovich and S. T. Sukhorukov, Preprint ITÉF-75, Institute of Theoretical and Experimental Physics, Moscow, 1978.
[66]L. D. Landau and E. M. Lifshitz, Kvantovaya mekhanika, Nauka, Moscow, 1974 (Quantum Mechanics–Non-Relativistic Theory, Pergamon Press, New York, 1977), §70.
[67]L. D. Landau, Sobranie trudov (Collected Works), Vol. 1, Nauka, Moscow, 1969, Article 8.
[68]J. G. Linhard, Cited in Ref. 45.
[69]P. Gratreau, Phys. Fluids **21**, 1302 (1978).
[70]B. A. Trubnikov, in: Fizika plazmy i problema UTR, Vol. 4, p. 87 (Plasma Physics and the Problem of Controlled Thermonuclear Reactions, Vol. 4, Pergamon Press, New York, 1961).
[71]J. Fukai and E. J. Clothiaux, Phys. Rev. Lett. **34**, 863 (1975).
[72]G. I. Budker, At. Energ. **5**, 9 (1956).
[73]V. V. Vikhrev and V. M. Korzhavin, Fiz. Plazmy **1**, 458 (1975) [Sov. J. Plasma Phys. **1**, 254 (1975)].
[74]L. D. Landau and E. M. Lifshitz, Teoriya polya, Nauka, Moscow, 1973 (The Classical Theory of Fields, Addison–Wesley, Reading, Mass., 1960).
[75]L. D. Landau and E. M. Lifshitz, Statisticheskaya fizika, Nauka, Moscow, 1976, Part 1 (Statistical Physics, Addison–Wesley, Reading, Mass.).
[76]V. B. Berestetskiĭ, E. M. Lifshitz, and L. P. Pitaevskiĭ, Relyativist-skaya kvantovaya teoriya (Relativistic Quantum Theory), Nauka, Moscow, 1968, Part 1.
[77]E. P. Lee, Phys. Fluids **21**, 1327 (1978).
[78]E. J. Lauer, R. J. Briggs, T. J. Fessenden, R. E. Hester, and E. P. Lee, Phys. Fluids **21**, 1344 (1978).
[79]A. A. Ivanov and L. I. Rudakov, Zh. Eksp. Teor. Fiz. **58**, 1332 (1970) [Sov. Phys. JETP **31**, 715 (1970)].
[80]R. S. Pease, Proc. R. Soc. London, Ser. B **70**, 11 (1957).
[81]S. I. Braginskiĭ, Zh. Eksp. Teor. Fiz. **33**, 645 (1957) [Sov. Phys. JETP **6**, 494 (1958)].
[82]J. D. Lawson, J. Nucl. Energy **C1**, 31 (1959).
[83]J. W. Shearer, Phys. Fluids **19**, 1426 (1976).
[84]V. V. Vikhrev, Pis'ma Zh. Eksp. Teor. Fiz. **27**, 104 (1978) [JETP Lett. **27**, 95 (1978)].
[85]D. J. Johnson, J. Appl. Phys. **45**, 1147 (1974).
[86]A. A. Aleksandrov, V. Gribkov, *et al.*, Kratkie Soobshcheniya po Fizike No. 3, 26 (1977).
[87]G. I. Budker, Cited in Ref. 70, Vol. 1, p. 243.

Translated by Dave Parsons